# The tumor suppressive TGF- /SMAD1/S1PR2 signaling axis is recurrently inactivated in diffuse large B-cell lymphoma

Stelling, Anna ; Hashwah, Hind ; Bertram, Katrin ; Manz, Markus G ; Tzankov, Alexandar ; Müller, Anne

Abstract: The sphingosine-1-phosphate receptor S1PR2 and its downstream signaling pathway is commonly silenced in diffuse large B-cell lymphoma (DLBCL), either by mutational inactivation or through negative regulation by the oncogenic transcription factor FOXP1. In this study, we have examined the upstream regulators of S1PR2 expression and have newly identified the TGF- /TGF- R2/SMAD1 axis as critically involved in S1PR2 transcriptional activation. Phosphorylated SMAD1 directly binds to regulatory elements in the locus as assessed by chromatin immunoprecipitation, and the CRISPR-mediated genomic editing of , or in DLBCL cell lines renders cells unresponsive to TGF- -induced apoptosis. DLBCL clones lacking any one of the three factors have a clear growth advantage in vitro, as well as in subcutaneous xenotransplantation models, and in a novel model of orthotopic growth of DLBCL cells in the spleens and bone marrow of MISTRG mice expressing various human cytokines. The loss of induces hyper-proliferation of the germinal center B-cell compartment of immunized mice and accelerates -driven lymphomagenesis in spontaneous and serial transplantation models. The specific loss of in murine GC B-cells phenocopies the effects of loss on GC B-cell hyper-proliferation. Finally, we show that SMAD1 expression is aberrantly downregulated in >85% of analyzed DLBCL patients. The combined results uncover an important novel tumor suppressive function of the TGF- /TGF- R2/SMAD1/S1PR2 axis in DLBCL, and show that DLBCL cells have evolved to inactivate the pathway at the level of SMAD1 expression.

DOI: https://doi.org/10.1182/blood-2017-10-810630

Blood First Edition Paper, prepublished online April 3, 2018; DOI 10.1182/blood-2017-10-810630

# The tumor suppressive TGF-β/SMAD1/S1PR2 signaling axis is recurrently inactivated in diffuse large B-cell lymphoma

Anna Stelling[1], Hind Hashwah[1], Katrin Bertram[1], Markus G. Manz[2], Alexandar Tzankov[3], and Anne Müller[1]

[1]Institute of Molecular Cancer Research and [2]Department of Hematology, University of Zürich, 8057 Zürich, Switzerland

[3]Institute of Pathology, University Hospital Basel, 4031 Basel, Switzerland

Correspondence: Anne Müller, Institute of Molecular Cancer Research, University of Zürich, Winterthurerstr. 180, 8057 Zürich, Switzerland. phone: +41 44 635 3474, fax: +41 44 635 3484, email: mueller@imcr.uzh.ch

**Running head: SMAD1 loss prevents TGF-β/S1PR2-driven apoptosis in DLBCL**

Abstract word count: 233

Text word count: 4486

Number of figures: 7

References: 35

Scientific category: LYMPHOID NEOPLASIA

**Key points:**

**-**The sphingosine-1-phosphate receptor 2 (S1PR2) is a *bona fide* tumor suppressor and transcriptionally regulated by the TGF-β/TGF-βR2/SMAD1 axis

-The aberrant loss of SMAD1 expression is very common in DLBCL and provides a proliferative advantage to B-cells *in vitro* and *in vivo*

**Abbreviations:** ChIP, chromatin immunoprecipitation; DLBCL, diffuse large B-cell lymphoma; FOXP1, forkhead box protein 1; SMAD, small mothers against decapentaplegic.

## Abstract

The sphingosine-1-phosphate receptor S1PR2 and its downstream signaling pathway is commonly silenced in diffuse large B-cell lymphoma (DLBCL), either by mutational inactivation or through negative regulation by the oncogenic transcription factor FOXP1. In this study, we have examined the upstream regulators of S1PR2 expression and have newly identified the TGF-β/TGF-βR2/SMAD1 axis as critically involved in S1PR2 transcriptional activation. Phosphorylated SMAD1 directly binds to regulatory elements in the *S1PR2* locus as assessed by chromatin immunoprecipitation, and the CRISPR-mediated genomic editing of *S1PR2*, *SMAD1* or *TGFBR2* in DLBCL cell lines renders cells unresponsive to TGF-β-induced apoptosis. DLBCL clones lacking any one of the three factors have a clear growth advantage *in vitro*, as well as in subcutaneous xenotransplantation models, and in a novel model of orthotopic growth of DLBCL cells in the spleens and bone marrow of MISTRG mice expressing various human cytokines. The loss of *S1pr2* induces hyper-proliferation of the germinal center B-cell compartment of immunized mice and accelerates *MYC*-driven lymphomagenesis in spontaneous and serial transplantation models. The specific loss of *Tgfbr2* in murine GC B-cells phenocopies the effects of *S1pr2* loss on GC B-cell hyper-proliferation. Finally, we show that SMAD1 expression is aberrantly downregulated in >85% of analyzed DLBCL patients. The combined results uncover an important novel tumor suppressive function of the TGF-β/TGF-βR2/SMAD1/S1PR2 axis in DLBCL, and show that DLBCL cells have evolved to inactivate the pathway at the level of SMAD1 expression.

## Introduction

Diffuse large B-cell lymphoma (DLBCL) is the most commonly diagnosed lymphoma in adults. It arises *de novo* at nodal or extranodal sites or as a consequence of high-grade transformation of indolent lymphomas or leukemias such as follicular lymphoma, chronic lymphocytic leukemia (CLL) and marginal zone lymphoma (MZL).[1,2,3] DLBCL represents a heterogeneous disease with molecular subtypes characterized by distinct gene expression profiles, specific sets of somatic mutations and differentially active intracellular signaling pathways.[4] Three subtypes of DLBCL can be distinguished based on their gene-expression similarities to their presumed normal B-cell counterparts, with activated B-cell-like (ABC) DLBCL resembling the post-germinal center plasmablast, germinal center B-cell-like (GCB) DLBCL deriving from GC B-cells and primary mediastinal B-cell lymphoma (PMBL) arising from a rare subset of thymic B-cells.[5,6] One of the biomarkers that is used to discriminate between GCB and ABC DLBCL is the Forkhead Box Protein 1 (FOXP1), a transcription factor that is highly expressed in the ABC subtype and is associated with poor prognosis.[7,8,9] FOXP1 predominantly functions as a repressor of protein-coding genes, several of which have documented tumor suppressive activities in B-cells.[10,11,12] We have recently identified the sphingosine 1-phosphate receptor 2 (S1PR2) as being negatively regulated by FOXP1 in ABC-DLBCL; its expression was inversely correlated with FOXP1 expression in a large cohort of DLBCL patients and was restored in DLBCL cell lines upon depletion of FOXP1.[10] Thus, S1PR2 is aberrantly silenced due to FOXP1 overexpression in ABC-DLBCL; conversely, in GCB-DLBCL, the *S1PR2* locus is subject to recurrent mutations that typically affect one of the two alleles.[13] Therefore, the two main DLBCL subtypes have evolved distinct mechanisms of silencing S1PR2 expression, both of which result in inactivation of the downstream signaling pathway involving the small G-protein Gα13 (encoded by the

*GNA13* gene), Rho and possibly the kinase AKT. The S1PR2/Gα13/AKT signaling axis has been implicated in the regulation of GC B-cell growth and dissemination.[13] Several pieces of evidence indicate that S1PR2 serves as a *bona fide* tumor suppressor in DLBCL: (1) the forced, doxycycline-induced expression of S1PR2 in DLBCL xenografts strongly delays tumor outgrowth, (2) the loss of one *S1PR2* allele is sufficient to predispose mice to c-*MYC*-driven lymphomagenesis, and (3) low S1PR2 expression, independently and in conjunction with high FOXP1 expression, represents a strong negative prognosticator of survival in patients with either subtype of DLBCL.[10]

In this study, we have addressed the consequences of S1PR2 inactivation for normal and malignant B-cell fate and have investigated the mechanisms of S1PR2 regulation in normal B-cells and in DLBCL. We show that the mutational inactivation of the *S1PR2* locus by CRISPR/Cas9 provides a major proliferative advantage to DLBCL cell lines *in vitro* and in xenotransplantation models, and that the loss of one or both alleles of *S1pr2* in murine GC B-cells promotes hyper-proliferation of the GC compartment upon sheep red blood cell immunization. We further provide evidence in various cell culture, xenotransplantation and genetically manipulated mouse models of the tumor suppressive activity of a newly identified TGF-βR2/SMAD1/S1PR2 axis in DLBCL.

## Methods

### Cell culture

The panel of DLBCL cell lines used here includes four of GCB DLBCL subtype (SU-DHL-6, SU-DHL-16, SU-DHL5 and RC-K8) and two of ABC DLBCL subtype (OCI-Ly3, OCI-Ly10). Cell lines were subjected to human TGF-β-1 (referred to as TGF-β) (PreproTech) treatment at various concentrations and analyzed with respect to cell viability, apoptosis, S1PR2 expression by qRT-PCR, transcription factor binding to the *S1PR2* promoter region by ChIP and protein expression by Western blot. Culture conditions, TGF-β treatment conditions, cell viability, proliferation and apoptosis assays, RNA extraction and qRT-PCR, siRNA transfections, CRISPR manipulations, ChIP-PCR and Western blotting techniques are all described in the supplemental methods.

### Animal experimentation

NOD/SCID/IL2Rγ$^{-/-}$ (NSG) mice and CSF$^{h}$;IL-3/GM-CSF$^{h}$;hSIRPA$^{tg}$;TPO$^{h}$;Rag2$^{-}$;γc$^{-}$ (MISTRG) mice[14] were obtained from a local repository. *Tgfbr2*$^{fl/fl}$ mice (B6;129-Tgfbr2tm1Karl/J) were crossed with AID-*Cre* mice (B6;FVB-Tg(Aicda-cre)1Rcas/J, both from the Jackson Laboratories). *S1pr2*$^{-/-}$ mice[15] were crossed with Emu-*MYC* mice expressing the *c-MYC* oncogene under the control of the Ig heavy chain enhancer (B6.Cg-Tg(IghMyc)22Bri/J, also from Jackson Laboratories)[16] to obtain composite strains. For induction of germinal centers, 6-8 week old mice were intraperitoneally immunized twice with a 10 day interval with 200µl of 10% sheep red blood cells (Innovative Research, Michigan, USA) and sacrificed 10 days after the last immunization. Spleens were processed and subjected to flow cytometric analysis. All flow

cytometry and staining procedures are described in the supplemental methods. *MYC*$^{tg}$ mice were examined and palpated two to three times weekly in order to detect signs of lymph node enlargement. Mice were sacrificed within 1 week of developing palpable tumors. Tumor cells pooled from the axillary and inguinal lymph nodes were cryopreserved in FCS with 10% DMSO. For serial transplantation studies, $1x10^6$ cells were injected intravenously into wildtype BL6 mice in a volume of 100 µl. Mice were palpated every other day for signs of lymph node engraftment. For xenotransplantation studies, CRISPR clones or wildtype RC-K8 or SU-DHL-6 ($10x10^6$ cells in 200µl PBS) were injected subcutaneously into both flanks of 6-8 week old NSG mice, or intravenously in a volume of 100µl into 6-8 weeks old MISTRG mice for orthotopic growth. Once palpable tumors had formed in the subcutaneous model, the volume of the tumors was measured by calipers and calculated using the formula (A2xB)/2, where A is the shorter and B the longer tumor dimension. Once palpable, wildtype SU-DHL-6 tumors were treated every 72 hours with 0.2µg human TGF-β (PreproTech) in a volume of 50µl reconstituted in 10mM Citric Acid and diluted in 0.1% BSA in 1x PBS. Control tumors were treated with 50µl 10mM Citric Acid/0.1% BSA diluted in 1x PBS. Intravenously injected mice were monitored three times a week for weight loss and other symptoms of disease. All animal studies were reviewed and approved by the Zürich Cantonal Veterinary Office (licenses 224/2014, 227/2015, 235/2015).

**Patient cohorts and SMAD1 immunohistochemistry**

Expression of SMAD1 was studied by immunohistochemistry on a phenotypically and genotypically well characterized collective of 76 patients uniformly treated with R-CHOP-14 and prospectively followed-up in the Swiss Group for Clinical Cancer Research 38/07 clinical

trial (ClinicalTrials.gov NCT00544219)[17] and on a retrospective collective of 184 primary DLBCL treated with rituximab-free regimens (mainly CHOP),[18] of which 74 patients had complete (and compatible with the formers') follow-up data. The primary polyclonal antibody (CellSignaling cs9743) was diluted 1:40 and incubated for 20 minutes in an automated immunostainer (Benchmark, Ventana/Roche) after heat-induced antigen retrieval with the CC1 buffer for 40 minutes.

**Statistics**

All statistical analyses were performed using Graph Pad Prism software. Graphs represent means plus SEM of at least two independent experiments for cell culture work and medians for mouse experiments unless otherwise indicated in the figure legend. Statistical analysis was performed using two-tailed student's t-test for *in vitro* assays, and using two-tailed Mann-Whitney test for *in vivo* studies as well as two-tailed Fisher's exact test for correlations of mutational status and SMAD1 expression in the patient cohort.

## Results

**Deletion of *S1PR2* by CRISPR/Cas9 confers a strong growth advantage to DLBCL cell lines *in vitro* and *in vivo*.** To confirm the putative tumor suppressive properties of S1PR2 in DLBCL, we used CRISPR to delete one or both alleles of the *S1PR2* locus in a cell line that is particularly suitable for this purpose due to its low FOXP1 and corresponding high S1PR2 expression (RC-K8; suppl. Figure 1A-B). Of the five S1PRs (S1PR1-5), only S1PR2 is expressed in DLBCL cells and controlled by FOXP1 expression (suppl. Figure 1C). Sequencing of the *S1PR2* and the *GNA13* genomic loci confirmed that both loci carry the wild type sequence in RC-K8 cells (suppl. Figure 1D). A CRISPR strategy (suppl. Figure 1E) was then used to delete the single *S1PR2* exon in one or both alleles of the locus (suppl. Figure 1F). Three $S1PR2^{+/-}$ and two $S1PR2^{-/-}$ clones were grown from FACS-sorted single cells and compared with respect to their *in vitro* growth to three wildtype clones ($S1PR2^{+/+}$) that had been subjected to the same electroporation and sorting procedures. Mono- and bi-allelically mutated clones exhibited a robust growth advantage over wildtype clones *in vitro* (Figure 1A); the same observation was made with $S1PR2^{-/-}$ clones generated using a second cell line (SU-DHL-6, Figure 1B). To address whether the growth advantage of $S1PR2^{-/-}$ clones was due to reduced apoptosis or due to enhanced proliferation, we flow cytometrically quantified the surface AnnexinV and nuclear Ki67 expression at various time points of the growth curve. Whereas apoptosis rates were similar across clones as determined by AnnexinV staining, $S1PR2^{-/-}$ clones showed significantly stronger Ki67 staining than $S1PR2^{+/+}$ clones (suppl. Figure 1G,H). $S1PR2^{+/-}$ and $S1PR2^{-/-}$ clones further also grew faster and formed larger tumors at the study end point compared to wildtype clones in a subcutaneous xenograft model of RC-K8 (Figure 1C-E). The NOD/SCID/IL2R$\gamma^{-/-}$ (NSG) mice used for subcutaneous xenotransplantation do not support orthotopic growth of

DLBCL cell lines upon intravenous (i.v.) injection. We instead turned to an alternative immunodeficient mouse developed on the Rag2$^{-/-}$IL2Rγ$^{-/-}$ background, termed MISTRG, which expresses the human cytokines M-CSF, IL-3, thrombopoietin, GM-CSF as well as SIRP1α, from the respective murine loci[19] and is known to support improved (orthotopic) growth of various myeloid neoplasias and solid tumors.[20,14,21] MISTRG mice supported the efficient engraftment of SU-DHL-6 cells, which grew in bone marrow and spleen; interestingly, *S1PR2*-mutant SU-DHL-6 clones grew more rapidly in both bone marrow and spleen than wildtype clones, accounting for the higher frequencies of human cells identified by FACS in these organs (Figure 1F-H, suppl. Figure 1I). The combined data indicates that S1PR2 expression restricts tumor cell proliferation in a cell-autonomous manner, further supporting the concept that S1PR2 is a *bona fide* tumor suppressor in DLBCL.

**Loss of *S1pr2* promotes hyper-proliferation of the germinal center B-cell compartment and increases lymphoma incidence in a spontaneous and a serial transplantation mouse model of DLBCL.** DLBCL arises from germinal center and post-germinal center (GC) B-cells that reside in secondary lymphoid organs or in lymphoid tissues at extranodal sites. To address whether the expression of S1PR2 affects GC formation and GC B-cell proliferation, we immunized wildtype or *S1pr2*$^{+/-}$ mice with two doses of sheep red blood cells (SRBCs) and flow cytometrically quantified GC B cells, centrocytes and centroblasts in the spleen at the study end point. The frequencies and absolute numbers of centrocytes, centroblasts, and of all GC B-cells were increased in *S1pr2*$^{+/-}$ mice (Figure 2A-C, suppl. Figure 2A-D). The increase in GC B-cells could be attributed to an increase in the size of individual GCs, but not their multiplicity per spleen, as determined by Ki67 staining of spleen sections (Figure 2D-F, suppl. Figure 2E). As

previously observed in a small preliminary cohort,[10] we confirmed that mice harboring a heterozygous *S1pr2* mutation with an additional *c-MYC* transgene under the B-cell-specific immunoglobulin heavy chain enhancer showed accelerated lymphoma development compared to *S1pr2*-proficient mice harboring the *c-MYC* transgene (suppl. Figure 2F). When lymph node cells from $S1pr2^{+/-}$ or $S1pr2^{+/+}$ *c-MYC*-transgenic mice were serially transplanted into wildtype mice we observed faster lymphoma development with transplanted $S1pr2^{+/-}$ cells relative to wildtype cells in recipient mice (Figure 2G-H, suppl. Figure 2G-H). These results suggest that S1PR2 controls GC B-cell proliferation and that the hyper-proliferation of GC B-cells due to loss of *S1pr2* may represent an early, initiating event in lymphomagenesis.

**S1PR2 expression is regulated by TGF-β and SMAD signaling.** We have previously shown that FOXP1 represses transcription at the *S1PR2* locus by binding to two regulatory elements located 2.5 (referred to as S1PR2 H) and 5 kb (S1PR2 G) upstream of the transcription start site.[10] However, little is known regarding activating transcription factors that regulate S1PR2 expression. We therefore screened several cytokines known to affect normal B-cell biology for their effects on S1PR2 expression and found that the addition of TGF-β, but not of IL-3, IL-5 or IL-6, dose-dependently induced the expression of S1PR2 in a subset of cell lines analyzed (Figure 3A, suppl. Figure 3A,B), with SU-DHL-6 and Oci-Ly10 showing the strongest response, RC-K8 and Oci-Ly3 being completely unresponsive to TGF-β and SU-DHL-16 and SU-DHL-5 showing a partial response. The effect of TGF-β was particularly strong when FOXP1 was simultaneously depleted by siRNAs (Figure 3B, suppl. Figure 3C); of note, TGF-β exposure had no effect on FOXP1 levels (suppl. Figure 3D), ruling out an indirect effect of TGF-β on S1PR2

expression via regulation of FOXP1. To examine which components of the TGF-β signaling pathway control the differential susceptibility of DLBCL cell lines to TGF-β treatment, we examined the expression of various SMAD transcription factors that were previously found to trans-activate target genes of the pathway in DLBCL.[22] Whereas SMAD9 was not expressed in any of the cell lines and SMAD5 was expressed in both highly and moderately responsive cell lines, the expression of SMAD1 was selectively detected only in those cell lines that showed strong responses to TGF-β and strong SMAD1/5/9 phosphorylation (Figure 3C, suppl. Figure 3E). We further examined the expression of the TGFβ receptor II (TGF-βR2) and found it to be universally expressed in all cell lines (Figure 3D, suppl. Figure 3F).

To address whether the SMAD proteins bind to regulatory elements of the *S1PR2* locus, we performed chromatin immunoprecipitation (ChIP) followed by qPCR specific for the regions 2.5 (H) and 5 kb (G) upstream of the *S1PR2* transcription start site. SMADs 1, 5 and 9 are all phosphorylated on serine residues by the active (ligand-bound) TGF-β receptor complex (consisting of type I and II receptor heterotetramer), which promotes the nuclear translocation of the complex and binding to chromatin. We therefore used a pSMAD1/5/9-specific antibody for ChIP, and found that pSMAD1/5/9 indeed precipitated with *S1PR2* genomic DNA, especially when cells were exposed to TGF-β for 4 hours prior to ChIP; this effect was observed in the TGFβ-responsive cell lines SU-DHL-6 and Oci-Ly10, but not the resistant cell lines RC-K8 and Oci-Ly3 (Figure 3E). Speculating that FOXP1 and SMAD1 interact directly at the *S1PR2* promoter, we immunoprecipitated FOXP1 and checked for a possible co-precipitation of SMAD1; however, no evidence could be found to that end in a cell line that co-expresses both proteins (suppl. Figure 3G).

As S1PR2 signaling has previously been shown to inhibit AKT phosphorylation and AKT-driven migration,[13] we speculated that TGF-β/SMAD1-induced S1PR2 expression might impair DLBCL cell survival by preventing AKT-mediated survival signaling. However, TGF-β treatment failed to affect AKT activation, as assessed by its auto-phosphorylation on serine 473, and also did not change overall AKT levels (suppl. Figure 3D) and thus does not appear to act through this pathway. The combined results indicate that TGF-β activates S1PR2 expression, especially if the repressor FOXP1 is removed, and implicate the non-canonical TGF-βR2/SMAD1/5/9 pathway, and in particular SMAD1, in the transcriptional activation of S1PR2.

**TGF-β induces S1PR2-dependent apoptosis in DLBCL cell lines *in vitro* and *in vivo*.** We have shown in a previous study that forced S1PR2 expression kills DLBCL cell lines both in culture and in xenotransplantation models.[10] To address whether TGF-β exposure and the concomitant endogenous S1PR2 upregulation is toxic to DLBCL cell lines, we treated cell lines showing differential responses to TGF-β (Figure 3A,C) with increasing doses of the cytokine. TGF-β exposure efficiently reduced cell viability and increased apoptosis dose-dependently; this effect was restricted to cell lines that upregulate S1PR2 upon TGF-β exposure and that are positive for SMAD1 (Figure 4A, suppl. Figure 4A,B). The effect was again particularly strong when FOXP1 was simultaneously depleted by siRNAs (Figure 4B). SU-DHL-6 clones that had been subjected to *S1PR2* deletion failed to undergo apoptosis upon TGF-β exposure, suggesting a critical role of S1PR2 in TGF-β driven apoptosis (Figure 4C). The TGF-β-sensitive cell line SU-DHL-6 was further assessed with respect to its susceptibility to TGF-β treatment in a xenograft model. Regular doses of intratumorally administered TGF-β resulted in lower tumor volumes and increased S1PR2 expression at the study endpoint relative to the vehicle control

(Figure 4D-F, suppl. Figure 4C). The combined results indicate that TGF-β signaling is cytotoxic for DLBCL cells *in vitro* and *in vivo*, and suggest that the apoptosis-promoting activity of TGF-β requires S1PR2.

**Loss of TGF-β signaling in the GC compartment induces GC B-cell hyper-proliferation.** To address in a genetic model whether the cell-intrinsic loss of TGF-β signaling in the GC B-cell compartment affects the GC reaction, we crossed *Tgfbr2*$^{fl/fl}$ mice with animals expressing Cre recombinase under the control of the GC-specific activation-induced cytidine deaminase promoter (*AID*-Cre). Mice lacking TGF-βR2 specifically in GC B-cells exhibited hyper-proliferation of their GC B-cells, centroblasts and centrocytes upon one round of SRBC immunization (Figure 5A-C, suppl. Figure 5A-C) and thus phenocopied the loss of S1PR2 in this compartment. The overall increase in GC cells could be attributed to an increase in the size of individual GCs, but not of their multiplicity per spleen, as determined by Ki67 staining of spleen sections (Figure 5D,E, suppl. Figure 5D). Together, the results demonstrate a critical role of the TGF-βR2/SMAD1/S1PR2 axis in the physiological control of the GC reaction and show for the first time that GC B-cell intrinsic TGF-β signaling is required for GC confinement.

**TGF-β signaling via TGF-βR2 and SMAD1 controls the proliferation of DLBCL cells.** To examine the contribution of the TGF-βR2/SMAD1 axis to cell death signaling in DLBCL in more detail, we inactivated *SMAD1* and *TGFβR2* in the SU-DHL-6 cell line by editing their first exons (suppl. Figure 6A,B) and exposing several clones each to TGF-β. The loss of *SMAD1* and *TGFβR2* rendered clones resistant to TGF-β-induced apoptosis and reduced their S1PR2

expression (Figure 6A,B). The contribution of SMAD1 to TGF-β-induced apoptosis could further be confirmed by a SMAD1-specific siRNA (Figure 6C, suppl. Figure 6C-D). Clones lacking either *SMAD1* or *TGFβR2* grew faster than wild type clones and thus phenocopied the effect of *S1PR2* inactivation in terms of their growth advantage *in vitro* (Figure 6D). Clones lacking *SMAD1*, but not those lacking *TGFβR2*, also grew faster and formed larger tumors when growing as subcutaneous xenografts on the flanks of NSG mice (Figure 6E, suppl. Figure 6E) and both *SMAD1* and *TGFβR2* knockout clones engrafted more readily in the spleen and the bone marrow when injected i.v. into MISTRG mice (Figure 6F). Furthermore, analysis of SMAD1 expression in a panel of 11 DLBCL cell lines confirmed its expression only in two cell lines (suppl. Figure 6F). Correlation analysis in the cell line panel confirmed the negative correlation between FOXP1 and S1PR2 expression and showed a trend towards a positive correlation between SMAD1 and TGF-βR2 versus S1PR2 expression (suppl. Figure 6G). The combined results indicate that TGF-β signals via TGF-βR2 and SMAD1 to control S1PR2 expression and DLBCL survival *in vitro* and restrict tumor growth *in vivo*.

**The expression of SMAD1 is aberrantly downregulated in DLBCL patients.** To test the clinical relevance of our observations in two Swiss patient cohorts, we studied the expression of SMAD1 by immunohistochemistry performed on tissue microarrays. 75 patient samples of a uniformly R-CHOP treated collective and 184 patients of a CHOP-treated collective were evaluable. Only 7 of the 75 (9.3%) and 29 of the 184 patients (15.7%), respectively, were found to express SMAD1 in 10 to 90% of tumor cells (Figure 6G); in all other (negative) cases, internal positive controls (vessels) stained as expected, but the lymphoma cells did not show SMAD1 positivity. In contrast, SMAD1 staining of normal tonsil samples showed uniformly positive

SMAD1 expression in centrocytes, but not centroblasts (suppl. Figure 6H). In both cohorts, the fraction of SMAD1-positive cases was equally low in patients with GCB (15%) and non-GCB (ABC; 13%) DLBCL subtype. The results indicate that SMAD1 is selectively downregulated in DLBCL, irrespective of the subtype. Further analyses of SMAD1 expression in relation to clinical characteristic of the patients, and the mutational profiles of the tumors as assessed by targeted high-throughput sequencing of all exons or hotspots of 68 frequently mutated genes, revealed that SMAD1 was more commonly expressed in *CD79b* mutant cases (2/4 vs. 2/70, p=0.041), in female patients (in the respective collectives: 6/34 vs. 1/41, p=0.030 and 14/60 vs. 16/124, p=0.043) and, not statistically significant, in *MYD88* mutant cases (p=0.066). We also examined whether aberrant silencing of SMAD1 was more common in patients with wild type *GNA13* than in patients with mutations in this important downstream mediator of S1PR2 signaling. 13 of 75 analyzed patients (17.3%) exhibited *GNA13* mutations. Among *GNA13*-wild type tumors, 7 of 62 were positive for SMAD1 (11.2%), whereas 0 of 13 *GNA13*-mutant tumors were SMAD1-positive (0%). The difference was not statistically significant (p=0.25). In conclusion, SMAD1 expression is aberrantly silenced in a large majority of GCB and non-GCB DLBCL cases, which does not appear to be (inversely) correlated with inactivating mutations in the S1PR2/Gα13 signaling pathway.

## Discussion

A growing body of evidence implicates S1PR2 as a novel, and uniformly important, tumor suppressor that is mutationally or transcriptionally inactivated in both major subtypes of DLBCL. In the GC B-cell subtype, the *S1PR2* locus, as well as genes encoding downstream components of the signaling pathway such as *GNA13*, are subject to recurrent mutational inactivation.[13] In the ABC subtype arising from post-germinal center plasmablasts, S1PR2 is repressed due to high FOXP1 expression (Figure 7), with FOXP1 acting as a direct negative regulator of S1PR2 expression by binding to two elements in the promoter region of the *S1PR2* gene.[10] In this study, we uncover a third and very common mechanism of S1PR2 downregulation that affects >85% of our patient cohort and the majority of examined DLBCL cell lines and involves the aberrant silencing of SMAD1. In SMAD1-expressing DLBCL cells, SMAD1 functions alongside other components of the non-canonical SMAD1/5/9 signaling complex in relaying signals from the type II TGF-β receptor upon binding of its ligand TGF-β (Figure 7). Whereas the receptor itself is universally expressed on all examined cell lines in our panel and appears to not be the limiting factor restricting signaling activity of the pathway, SMAD1 expression is absent in the majority of our cell lines (and of our cohorts), possibly reflecting its transcriptional silencing by DNA methylation. The knock down of SMAD1 by RNAi, or the CRISPR-mediated editing and inactivation of the *SMAD1* gene in SMAD1-positive DLBCL cells, both inhibit TGF-β–dependent S1PR2 expression, indicating that SMAD1-negative cases of DLBCL likely are unresponsive to the pro-apoptotic activities of this cytokine *in vivo*. We indeed found in various xenotransplantation settings and under cell culture conditions, that SMAD1 and TGF-βR2 are not only required for S1PR2 expression, but also for the induction of apoptosis by TGF-β, which in turn was dependent on S1PR2 as judged by the pro-apoptotic

response of S1PR2-proficient but not –deficient DLBCL clones to TGF-β. DLBCL clones lacking SMAD1, or TGF-βR2, or S1PR2 expression all have a growth advantage over wildtype clones *in vitro* and *in vivo*. This effect was particularly evident in a novel model of orthotopic DLBCL growth that allows for efficient engraftment of various cell lines, including the SU-DHL-6 used here, in the spleen and bone marrow of MISTRG mice. The new model overcomes the current limitations in DLBCL research by providing a versatile, practical, fast and readily available model for *in vivo* work that, especially in combination with CRISPR manipulation of the transplanted cell lines, lends itself to multiple applications, including drug testing.

The observation that TGF-β activates non-canonical SMAD1/5/9 signaling via TGF-βR2 in normal B-cells and in various other cell types is not new,[23,24,25,26,27] and some evidence is available for the concept that this process is impaired in malignant B-cells. For example, in Burkitt lymphoma and in Epstein–Barr virus-transformed B-lymphoblastoid cell lines, reduced TGF-βR2 expression renders cells partially resistant to TGF-β.[28] Point mutations in TGF-βR2 were found to inhibit its tumor suppressive activities in cutaneous T-cell lymphoma.[29] Furthermore, TGF-βR2 expression has been proposed as a positive prognostic factor in DLBCL patients,[30] an observation that fits very well with our model. Large scale screening and drug testing efforts have identified the TGF-β signaling pathway as a promising target in DLBCL that may be exploited for chemo-sensitization purposes.[31,32,33] Our results thus provide a mechanistic link between two previously known or suspected tumor suppressive pathways frequently inactivated in DLBCL- one involving aberrant inactivation of S1PR2 signaling and its pro-apoptotic activities, and the other involving the TGF-β signaling pathway. SMAD1 links the two pathways by directly binding to the *S1PR2* promoter once it is phosphorylated by ligand-bound TGF-βR2 and has translocated to the nucleus.

Mechanistic evidence from animal models, presented here and in two previous studies,[34,35] suggests that S1PR2 inactivation represents an early event in DLBCL initiation. The loss of only one functional allele of *S1pr2* was sufficient to predispose mice to hyper-proliferation of the GC compartment upon immunization, a phenotype that was recapitulated by the loss of one or both copies of *Tgfbr2*. Both centrocytes and centroblasts were more numerous in the absence of *S1pr2* or *Tgfbr2* and their over-representation in splenocyte preparations could be linked to larger rather than more numerous GCs. The fact that there is no reliable S1PR2 antibody available did not allow us to confirm the decreased S1PR2 expression in heterozygous knockout mice, nevertheless the clear phenotype of these mice strongly suggests that the mice have a lower receptor expression upon loss of one copy of *S1pr2*. The fact that S1PR2 plays an important role in GC confinement has been shown previously[35] and has been linked to a gradient of S1P within the GC that prevents GC cells from prematurely exiting the compartment. Our data suggest that an additional layer of regulation exists that involves TGF-β acting further upstream within GC B-cells to control S1PR2 expression. This model is supported by the observations that tonsillar centrocytes, but not centroblasts express high levels of SMAD1, and that the S1PR2 repressor FOXP1 is downregulated in the GC B-cell compartment.[10]

Several lines of evidence suggest that S1PR2 acts cell-intrinsically in tumor B-cells, rather than in tumor-infiltrating non-malignant cells to promote cell death (for example in response to TGF-β) and/or to limit the proliferative capacities of normal and malignant B-cells. This model is supported by the hyper-proliferation of S1PR2-deficient DLBCL cells *in vitro* and *in vivo*, by the fact that MYC-expressing murine lymphoma cells, injected i.v. into wildtype recipient mice, form larger tumors in lymph nodes and spleen if they lack one copy of *S1pr2,* and by our previous observation that forced expression of S1PR2 reduces tumor size in established

lymphomas.[10] Patients with low S1PR2 expression have a significantly worse prognosis than patients with high S1PR2 expression, and the benefits of high S1PR2 expression are especially obvious in combination with low FOXP1 expression.[10] In summary, we show here for the first time that two major tumor suppressive pathways in DLBCL intersect at the level of the transcription factor SMAD1, which mediates pro-apoptotic TGF-β signaling by binding directly to the *S1PR2* promoter and thereby activating S1PR2 expression, a process that is particularly efficient in the absence of the repressor FOXP1 (Figure 7). In accordance with its critical role in TGF-β-driven apoptosis, SMAD1 expression is aberrantly low or absent in a large majority of DLBCL patients. The combined results reveal an important novel tumor suppressive function of the TGF-β/TGF-βR2/SMAD1/S1PR2 axis in DLBCL, and demonstrate for the first time that DLBCL cells have evolved to inactivate this cell death-promoting pathway at the level of SMAD1 expression.

## Acknowledgments

This study was funded by the Swiss Cancer Leagues grants KLS-3612-02-2015 and KFS-4120-02-2017 to A.M. Additional support was provided by the Clinical Research Priority Program "Human Hemato-lymphatic Diseases" of the University of Zurich. The authors wish to thank Michael Flori, Cheuk Ting Wu, Maries van den Broek and all consortium members of the Clinical Research Priority Program for support and helpful discussions.

## Authorship and conflict-of-interest statements

A.S. designed, performed and analyzed most of the experiments and co-wrote the manuscript; H.H. and K.B. helped with experiments and provided critical tools and advice. A.T. analyzed patient cohorts, M.G.M. provided critical tools and intellectual input and A.M. supervised the study and co-wrote the manuscript. The authors declare that no conflict of interest exists.

## References


1. Pasqualucci L, Khiabanian H, Fangazio M, et al. Genetics of Follicular Lymphoma Transformation. *Cell Rep.* 2014;6(1):130–140.

2. Schneider C, Pasqualucci L, Dalla-Favera R. Molecular Pathogenesis of Diffuse Large B-cell Lymphoma. *Semin Diagn PAtholChanges*. 2012;29(6):997–1003.

3. Shaffer 3rd AL, Young RM, Staudt LM. Pathogenesis of human B cell lymphomas. *Annu Rev Immunol*. 2012;30:565–610.

4. Roschewski M, Staudt LM, Wilson WH. Diffuse large B-cell lymphoma-treatment approaches in the molecular era. *Nat. Rev. Clin. Oncol.* 2014;11(1):12–23.

5. Alizadeh AA, Eisen MB, Davis RE, et al. Distinct types of diffuse large B-cell lymphoma identified by gene expression profiling. *Nature*. 2000;403(6769):503–511.

6. Rosenwald A, Wright G, Leroy K, et al. Molecular diagnosis of primary mediastinal B cell lymphoma identifies a clinically favorable subgroup of diffuse large B cell lymphoma related to Hodgkin lymphoma. *J. Exp. Med.* 2003;198(6):851–62.

7. Barrans SL, Fenton JA, Banham A, Owen RG, Jack AS. Strong expression of FOXP1 identifies a distinct subset of diffuse large B-cell lymphoma (DLBCL) patients with poor outcome. *Blood*. 2004;104(9):2933–2935.

8. Hoeller S, Schneider A, Haralambieva E, Dirnhofer S, Tzankov A. FOXP1 protein overexpression is associated with inferior outcome in nodal diffuse large B-cell lymphomas with non-germinal centre phenotype, independent of gains and structural aberrations at 3p14.1. *Histopathology*. 2010;57(1):73–80.

9. Tzankov A, Leu N, Muenst S, et al. Multiparameter analysis of homogeneously R-CHOP-treated diffuse large B cell lymphomas identifies CD5 and FOXP1 as relevant prognostic biomarkers: report of the prospective SAKK 38/07 study. *J Hematol Oncol*. 2015;8:70.

10. Flori M, Schmid CA, Sumrall ET, et al. The hematopoietic oncoprotein FOXP1 promotes tumor cell survival in diffuse large B-cell lymphoma by repressing S1PR2 signaling. *Blood*. 2016;127(11):1438–1448.

11. van Keimpema M, Gruneberg LJ, Mokry M, et al. FOXP1 directly represses transcription of proapoptotic genes and cooperates with NF-kappaB to promote survival of human B cells. *Blood*. 2014;124(23):3431–3440.

12. Wong KK, Gascoyne DM, Brown PJ, et al. Reciprocal expression of the endocytic protein HIP1R and its repressor FOXP1 predicts outcome in R-CHOP-treated diffuse large B-cell lymphoma patients. *Leuk. Off. J. Leuk. Soc. Am. Leuk. Res. Fund, U.K.* 2013;

13. Muppidi JR, Schmitz R, Green JA, et al. Loss of signalling via Galpha13 in germinal centre B-cell-derived lymphoma. *Nature*. 2014;516(7530):254–258.

14. Rongvaux A, Willinger T, Martinek J, et al. Development and function of human innate immune cells in a humanized mouse model. *Nat. Biotechnol.* 2014;32(4):364–72.

15. Kono M, Mi Y, Liu Y, et al. The sphingosine-1-phosphate receptors S1P1, S1P2, and S1P3 function coordinately during embryonic angiogenesis. *J. Biol. Chem.* 2004;279(28):29367–29373.

16. Adams JM, Harris AW, Pinkert CA, et al. The c-myc oncogene driven by immunoglobulin enhancers induces lymphoid malignancy in transgenic mice. *Nature*. 318(6046):533–8.

17. Juskevicius D, Jucker D, Klingbiel D, et al. Mutations of CREBBP and SOCS1 are independent prognostic factors in diffuse large B cell lymphoma: mutational analysis of the SAKK 38/07 prospective clinical trial cohort. *J. Hematol. Oncol.* 2017;10(1):70.

18. Muenst S, Hoeller S, Willi N, Dirnhofera S, Tzankov A. Diagnostic and prognostic utility of PD-1 in B cell lymphomas. *Dis. Markers*. 2010;29(1):47–53.

19. Rongvaux A, Takizawa H, Strowig T, et al. Human Hemato-Lymphoid System Mice: Current Use and Future Potential for Medicine. *Annu. Rev. Immunol.* 2013;31(1):635–674.

20. Ellegast JM, Rauch PJ, Kovtonyuk L V, et al. inv(16) and NPM1mut AMLs engraft human cytokine knock-in mice. *Blood*. 2016;128(17):2130–2134.

21. Theocharides APA, Rongvaux A, Fritsch K, Flavell RA, Manz MG. Humanized hemato-lymphoid system mice. *Haematologica*. 2016;101(1):5–19.

22. Rai D, Kim S-W, McKeller MR, Dahia PLM, Aguiar RCT. Targeting of SMAD5 links microRNA-155 to the TGF-beta pathway and lymphomagenesis. *Proc. Natl. Acad. Sci. U. S. A.* 2010;107(7):3111–6.

23. Bakkebø M, Huse K, Hilden VI, Smeland EB, Oksvold MP. TGF-β-induced growth inhibition in B-cell lymphoma correlates with Smad1/5 signalling and constitutively active p38 MAPK. *BMC Immunol.* 2010;11(1):57.

24. Jiang D, Aguiar RCT. MicroRNA-155 controls RB phosphorylation in normal and malignant B lymphocytes via the noncanonical TGF- b 1 / SMAD5 signaling module. *Blood*. 2016;123(1):86–94.

25. Munoz O, Fend F, de Beaumont R, et al. TGFbeta-mediated activation of Smad1 in B-cell non-Hodgkin's lymphoma and effect on cell proliferation. *Leukemia*. 2004;18(12):2015–25.

26. Daly AC, Randall RA, Hill CS. Transforming growth factor beta-induced Smad1/5 phosphorylation in epithelial cells is mediated by novel receptor complexes and is essential for anchorage-independent growth. *Mol. Cell. Biol.* 2008;28(22):6889–902.

27. Wrighton KH, Lin X, Yu PB, Feng X-H. Transforming Growth Factor β Can Stimulate Smad1 Phosphorylation Independently of Bone Morphogenic Protein Receptors. *J. Biol. Chem.* 2009;284(15):9755–9763.

28. Inman GJ, Allday MJ. Resistance to TGF- β 1 correlates with a reduction of TGF- β type II receptor expression in Burkitt ' s lymphoma and Epstein – Barr virus-transformed B lymphoblastoid cell lines. 2000;4(2000):1567–1578.

29. Knaus PI, Lindemann D, DeCoteau JF, et al. A dominant inhibitory mutant of the type II transforming growth factor beta receptor in the malignant progression of a cutaneous T-cell lymphoma. *Mol. Cell. Biol.* 1996;16(7):3480–9.

30. Mao S, Yang W, Ai L, Li Z, Jin J. Transforming growth factor β type II receptor as a marker in diffuse large B cell lymphoma. *Tumour Biol.* 2015;36(12):9903–8.

31. Camicia R, Winkler HC, Hassa PO. Novel drug targets for personalized precision medicine in relapsed/refractory diffuse large B-cell lymphoma: a comprehensive review. Molecular Cancer; 2015.

32. Clozel T, Yang S, Elstrom RL, et al. Mechanism-Based Epigenetic Chemosensitization Therapy of Diffuse Large B-Cell Lymphoma. *Cancer Discov.* 2013;3(9):1002–1019.

33. Pan H, Jiang Y, Boi M, et al. Epigenomic evolution in diffuse large B-cell lymphomas. *Nat. Commun.* 2015;6:6921.

34. Cattoretti G, Mandelbaum J, Lee N, et al. Targeted disruption of the S1P2 sphingosine 1-phosphate receptor gene leads to diffuse large B-cell lymphoma formation. *Cancer Res.* 2009;69(22):8686–8692.

35. Green JA, Suzuki K, Cho B, et al. The sphingosine 1-phosphate receptor S1P(2) maintains the homeostasis of germinal center B cells and promotes niche confinement. *Nat Immunol*. 2011;12(7):672–680.

## Figure Legends

**Figure 1. Genomic editing of the *S1PR2* locus provides a growth advantage to DLBCL cell lines *in vitro* and *in vivo*.** (A,B) The DLBCL cell lines RC-K8 (A) and SU-DHL-6 (B) were subjected to *S1PR2* inactivation using CRISPR/Cas9 editing. Absolute cell counts of two to three independent clones derived from FACS-sorted single cells of the indicated genotypes were compared under standard cell culture conditions over ten days without medium change. Pooled results from two out of a total of four independent experiments (A) and of four independent experiments (B) are shown. p-values were calculated using the student t- test on the average value for each genotype pooling $S1PR2^{+/-}$ and $S1PR2^{-/-}$ clones. (C-E) Ten million cells each of five $S1PR2^{+/+}$ clones (red), four $S1PR2^{+/-}$ clones (blue) and two $S1PR2^{-/-}$ clones (all in the RC-K8 cell line; black) were injected subcutaneously into the flanks of NSG mice. Tumors were excised, representative macroscopic images were taken (C), and tumor weights (D) and volumes (E) were determined at the study endpoint 40 days post injection. Every dot represents one tumor and plots show pooled data from two independent experiments. (F-H) Ten million cells per mouse of two to three replicates each of three independent $S1PR2^{+/+}$ clones (red) and three $S1PR2^{-/-}$ clones (all in the SU-DHL-6 cell line; black) were injected intravenously into MISTRG mice. Mice were sacrificed 35 days after tumor cell injection, their spleens were weighed (F) and the frequencies of $hCD45^{+}$ cells in the spleen (G) and the bone marrow (H) was determined by flow cytometry. Every dot represents one mouse and graphs represent pooled data from two independent experiments. In D-H, horizontal lines indicate medians and p-values were calculated using the Mann-Whitney test. *p<0.05; **p<0.01; ***p<0.001.

**Figure 2. The mono-allelic loss of *S1pr2* promotes hyper-proliferation of the germinal center B-cell compartment and increases the lymphoma burden in a spontaneous and a serial transplantation model of *MYC*-driven lymphomagenesis.** (A-F) *S1pr2*$^{+/+}$ and *S1pr2*$^{+/-}$ mice on the BL/6 background were immunized twice intraperitoneally with 200 µl 10% sheep red blood cells (SRBCs), with a ten day interval between the two immunizations. Mice were sacrificed ten days after the last immunization and GC B-cells were flow cytometrically identified as CD95$^{hi}$ CD38$^{lo}$ in the CD19$^{+}$ B-cell compartment (A-C). GC B-cell frequencies in % of all CD19$^{+}$ B-cells as well as absolute numbers per spleen are shown in A and B, alongside representative FACS plots in C. Non-immunized littermates are shown as control. (D-F) The GC area (arbitrary units) of immunized mice was determined by quantifying three Ki-67-stained spleen sections per mouse using ImageJ (D). Representative pictures of spleens of immunized *S1pr2*$^{+/+}$ and *S1pr2*$^{+/-}$ mice are shown in E and F. Size bar represents 1000µm; arrows point to GCs. Every dot in A, B and D represents one mouse and data from five pooled experiments are shown. (G,H) One million lymph node cells per mouse, harvested from three *S1pr2*$^{+/+}$ and three *S1pr2*$^{+/-}$ *MYC*$^{tg}$ donor mice of the cohorts shown in supplemental Figure 2F were injected intravenously into wildtype BL/6 recipients. Mice were palpated every other day for enlarged lymph nodes and sacrificed after 20 days, i.e. when the first mice showed disease symptoms. Spleen weights (G) and lymph node weights (H) were determined. Lymph node weights represent the average of two inguinal and two axillary lymph nodes. Control mice were not injected with tumor cells. In A, B, D, G and H, horizontal lines indicate medians and p-values were calculated using the Mann-Whitney test. *p<0.05; **p<0.01.

**Figure 3. S1PR2 expression is regulated by the TGF-β/SMAD signaling pathway.** (A) *S1PR2* expression after 24h of treatment with the indicated increasing doses of TGF-β, as assessed in the SU-DHL-6, Oci-Ly10, RC-K8 and Oci-Ly3 DLBCL cell lines by qRT-PCR. (B) The DLBCL cell line SU-DHL-6 was treated with FOXP1 targeting siRNA for 48h and subjected to treatment with 2 ng/ml TGF-β for an additional 24h. Data in A and B are pooled from three or more independent experiments. Graphs show mean +SEM; p-values were calculated using the student t-test. (C) The indicated DLBCL cell lines were treated with 2 ng/ml TGF-β for 1h and subjected to immunoblotting with antibodies against the indicated SMAD proteins, p-SMAD1/5/9 and tubulin. Representative immunoblots of at least two independent experiments are shown. (D) TGF-βR2 surface expression of the indicated DLBCL cell lines, as assessed by flow cytometry. The plots are representative for two independent experiments. (E) pSMAD1/5/9 ChIP of cells treated or not with 5 ng/ml TGF-β for 4h; an unspecific rbIgG antibody was used as control. Eluted DNA was subjected to PCR using primers amplifying two regions 2.5 and 5 kb upstream of the *S1PR2* TSS. MyoD was amplified as negative control; CDKN1A and ID1 were used as positive controls for canonical TGF-β and BMP signaling. Graphs represent the fold change of the yield relative to 1% input of the pSMAD1/5/9 sample versus rbIgG; means +SD of two independent experiments are shown. *p<0.05; **p<0.01; ***p<0.001; ****p<0.0001.

**Figure 4. TGF-β induces S1PR2-dependent apoptosis in DLBCL cell lines *in vitro* and *in vivo*.** (A) Cell viability and apoptosis, as determined by Cell Titer Blue assay and annexin V staining, of the indicated cell lines after 24h of exposure to increasing concentrations of TGF-β; values are normalized to the untreated control sample. (B) The DLBCL cell line SU-DHL-6 was

treated with FOXP1 targeting siRNA for 48h, subjected to 2 ng/ml TGF-β for additional 24h, and analyzed as described in A. Data in A and B are pooled from three or more independent experiments. Graphs show means +SEM; p-values were calculated using the student t-test. (C) Three *S1PR2*$^{+/+}$, one *S1PR2*$^{+/-}$ and three *S1PR2*$^{-/-}$ clones generated in the SU-DHL-6 cell line were treated with 2 ng/ml TGF-β and analyzed for apoptosis by annexinV staining. Bars represent pooled data for each genotype relative to the untreated control of each clone. Each clone was analyzed three to six times. Graphs represent means +SEM; p-values were calculated using the student t-test. (D-F) Ten million SU-DHL-6 cells were injected subcutaneously into both flanks of NSG mice. One tumor per mouse was injected intratumorally with TGF-β at the depicted intervals (D), and the other received vehicle only. Tumor volumes were measured after excision (E) and RNA was extracted and qRT-PCR for S1PR2 was performed on excised tumor tissue (F). In F, each dot represents one tumor and results are pooled from two independent experiments. S1PR2 expression analysis was only performed in one of the two studies with n=10 per group. Two control and one TGF-β-treated tumor had to be excluded due to insufficient RNA quality. TGF-β-treated and control tumors are compared for each mouse. p-values were calculated using the Mann-Whitney test. *p<0.05; **p<0.01; ***p<0.001; ****p<0.0001.

**Figure 5. Loss of TGF-β signaling in the GC compartment induces GC B-cell hyper-proliferation.** (A-E) *Tgfbr2*$^{fl/fl}$ mice were crossed with AID-*Cre* mice; *Tgfbr2*$^{wt/wt}$, *Tgfbr2*$^{fl/wt}$ and *Tgfbr2*$^{fl/fl}$ x AID-*Cre* mice were immunized intravenously with 200 µl 10% SRBCs, sacrificed ten days after immunization and GC cells were analyzed by flow cytometry as described in Figure 2. GC B-cell frequencies in % of all CD19$^{+}$ B-cells as well as absolute numbers per spleen are shown in A and B, alongside representative FACS plots in C. Non-immunized

littermates are shown as control. (D,E) The GC area (arbitrary units) of immunized mice was determined by quantifying three Ki-67-stained spleen sections per mouse using ImageJ (D). Representative pictures of spleens of immunized mice of the indicated genotypes are shown in E. Size bar represents 1000µm; arrows point to GCs. Every dot in A, B and D represents one mouse and data from three pooled experiments are shown. Graphs show Medians. *p<0.05; **p<0.01.

**Figure 6. TGF-β signaling via TGF-βR2 and SMAD1 activates S1PR2 expression and induces apoptosis of DLBCL cells and SMAD1 expression is downregulated in DLBCL patients.** (A) Three *SMAD1*$^{+/+}$ and two *SMAD1*$^{-/-}$ as well as three *TGFβR2*$^{+/+}$ and three *TGFβR2*$^{-/-}$ clones (all generated in the SU-DHL-6 cell line) were treated with 2 ng/ml TGFβ for 24 h and analyzed for apoptosis with annexin V staining. Bars represent pooled data for each genotype relative to the untreated control of each clone. (B) The same clones as in A were subjected to RNA extraction and S1PR2-specific qRT-PCR. Each clone in A and B was analyzed twice, graphs represent means +SEM; p-values were calculated using the student t-test. (C) The DLBCL cell line SU-DHL-6 was treated with SMAD1-targeting siRNA for 48h and subjected to 2 ng/ml TGFβ for additional 24h. Cells were analyzed for apoptosis by annexinV staining. Graphs show pooled results from six independent experiments. Means +SEM are represented. p-values were calculated using the student t-test. (D) Absolute cell counts of two to three independent clones derived from FACS-sorted single cells of the indicated genotypes were compared under standard cell culture conditions over ten days without medium change. Two experimental replicates are shown. p-values were calculated using the student t- test on the average value for each genotype. (E) Ten million cells each of three *SMAD1*$^{+/+}$ clones (grey), and two *SMAD1*$^{-/-}$ clones (red, in SU-DHL-6) were injected subcutaneously into the flanks of NSG

mice. Tumors were excised and tumor weights and tumor volumes were determined at the study endpoint 24 days after injection. Every dot represents one tumor and plots show pooled data from two independent experiments. (F) Ten million cells of six *SMAD1*/TGFβR2$^{+/+}$ clones (grey) and two *SMAD1*$^{-/-}$ (red) or three TGFβR2$^{-/-}$ (blue, all in SU-DHL-6) clones were injected intravenously into MISTRG mice. Mice were sacrificed 35 days post injection, their spleens were weighed and the frequencies of hCD45$^{+}$ cells in the spleens and bone marrow was determined by flow cytometry. Every dot represents one mouse and graphs represent data from three experiments. Horizontal lines in E and F indicate medians and p-values were calculated using the Mann-Whitney test. (G) Negative (left) and positive (right) SMAD1 immunohistochemical staining of DLBCL patient samples. Size bar represents 20μm *p<0.05; **p<0.01; ***p<0.001; ****p<0.0001.

**Figure 7. Schematic summarizing the tumor suppressive properties of the TGF-β/SMAD1/S1PR2 axis in DLBCL.** Under physiological conditions, centrocytes and centroblasts express large amounts of S1PR2, which promotes GC confinement due to a gradient of S1P that increases in concentration towards the borders of the GC and leads to apoptosis in GC cells that attempt to exit the GC. In DLBCL, S1PR2 is either mutated (in the GCB subtype) or transcriptionally downregulated by FOXP1 (in the ABC subtype). Loss of S1PR2 thus is an early initiating event in both major subtypes of DLBCL. The expression of S1PR2 is further regulated by TGF-β, which binds to its receptor TGF-βR2 and activates SMAD1 phosphorylation and nuclear translocation. p-SMAD1 binds directly to regulatory elements in the S1PR2 promoter and activates S1PR2 expression; most cases of DLBCL exhibit aberrantly low or absent expression of SMAD1.

# Figure 1

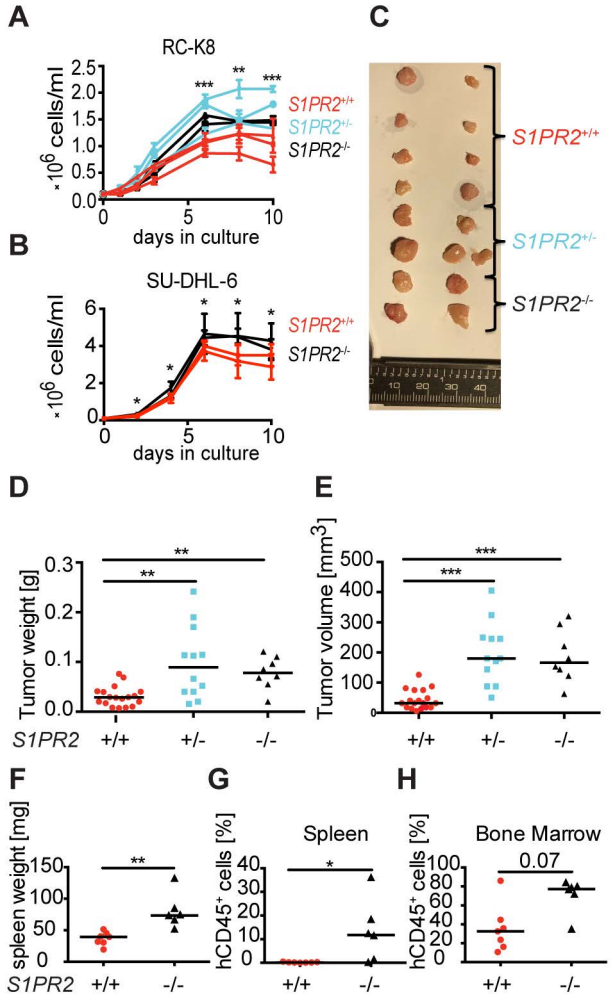
A
RC-K8
×10^6 cells/ml
days in culture
S1PR2+/+
S1PR2+/-
S1PR2-/-
B
SU-DHL-6
×10^6 cells/ml
days in culture
S1PR2+/+
S1PR2-/-
C
S1PR2+/+
S1PR2+/-
S1PR2-/-
D
Tumor weight [g]
S1PR2 +/+ +/- -/-
E
Tumor volume [mm3]
+/+ +/- -/-
F
spleen weight [mg]
S1PR2 +/+ -/-
G
Spleen
hCD45+ cells [%]
+/+ -/-
H
Bone Marrow
0.07
hCD45+ cells [%]
+/+ -/-

# Figure 2

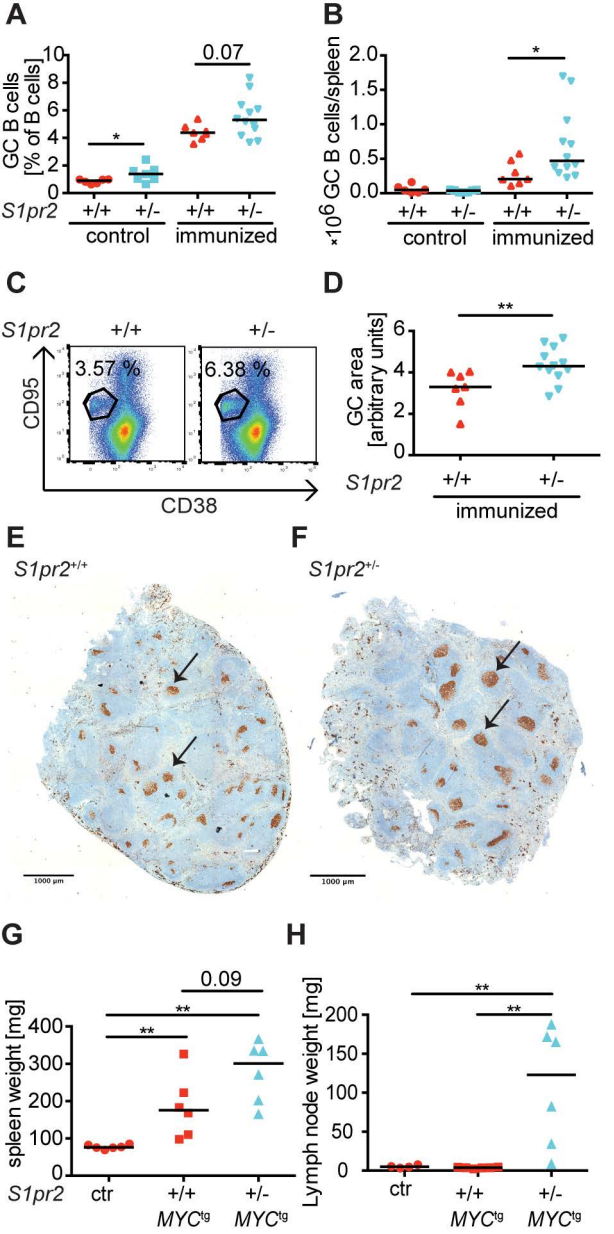
A
GC B cells [% of B cells]
0.07
*
S1pr2
+/+ +/- +/+ +/-
control immunized
B
×10^6 GC B cells/spleen
*
+/+ +/- +/+ +/-
control immunized
C
S1pr2 +/+ +/-
3.57 %
6.38 %
CD95
CD38
D
GC area [arbitrary units]
**
S1pr2 +/+ +/-
immunized
E
S1pr2+/+
F
S1pr2+/-
1000 µm
1000 µm
G
spleen weight [mg]
0.09
**
**
S1pr2 ctr +/+ MYCtg +/- MYCtg
H
Lymph node weight [mg]
**
**
ctr +/+ MYCtg +/- MYCtg

Figure 3

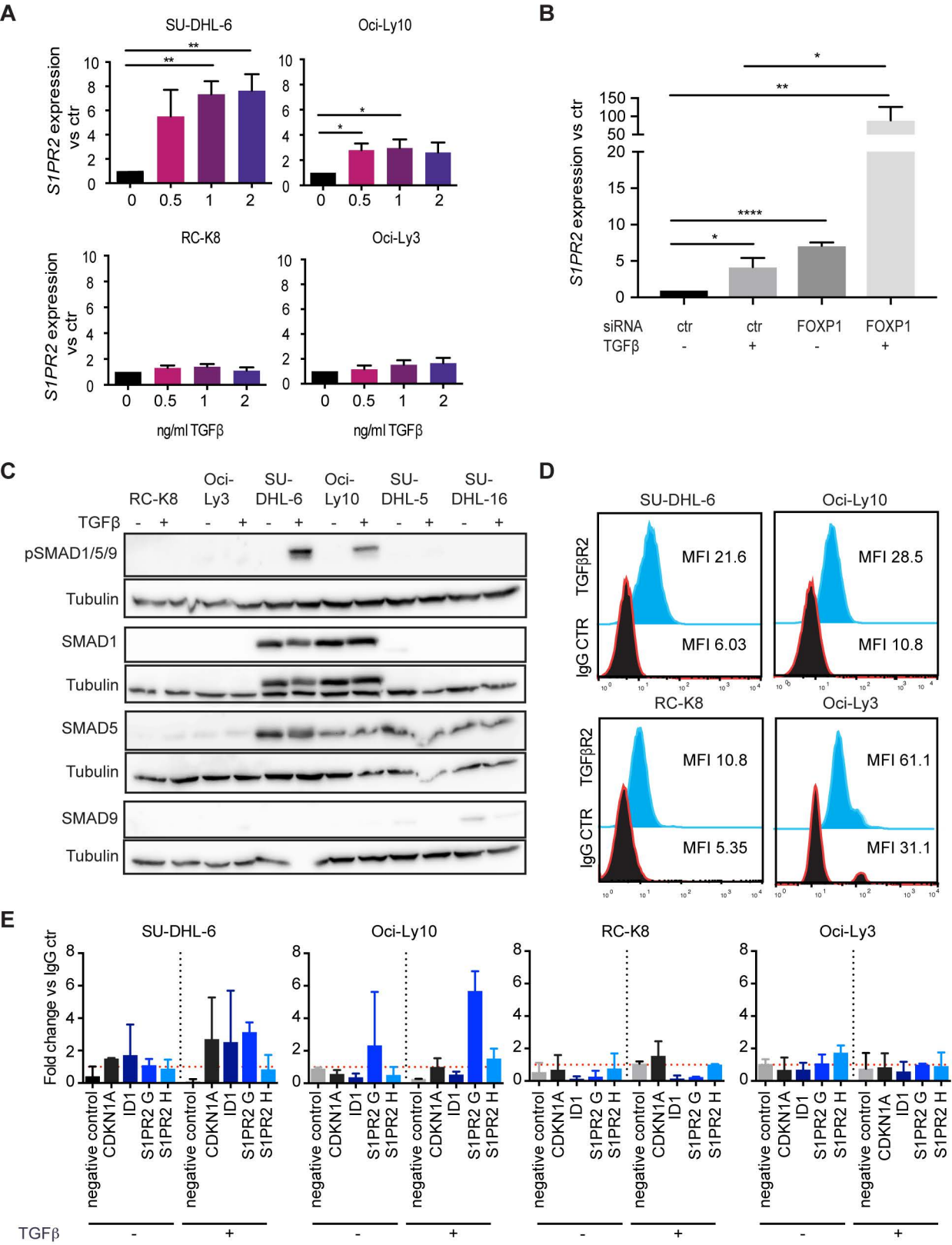
A
SU-DHL-6
Oci-Ly10
RC-K8
Oci-Ly3
S1PR2 expression vs ctr
ng/ml TGFβ
B
S1PR2 expression vs ctr
siRNA
ctr
FOXP1
TGFβ
C
RC-K8
Oci-Ly3
SU-DHL-6
Oci-Ly10
SU-DHL-5
SU-DHL-16
TGFβ
pSMAD1/5/9
Tubulin
SMAD1
SMAD5
SMAD9
D
SU-DHL-6
Oci-Ly10
RC-K8
Oci-Ly3
TGFβR2
IgG CTR
MFI 21.6
MFI 6.03
MFI 28.5
MFI 10.8
MFI 10.8
MFI 5.35
MFI 61.1
MFI 31.1
E
Fold change vs IgG ctr
negative control
CDKN1A
ID1
S1PR2 G
S1PR2 H
TGFβ

# Figure 4

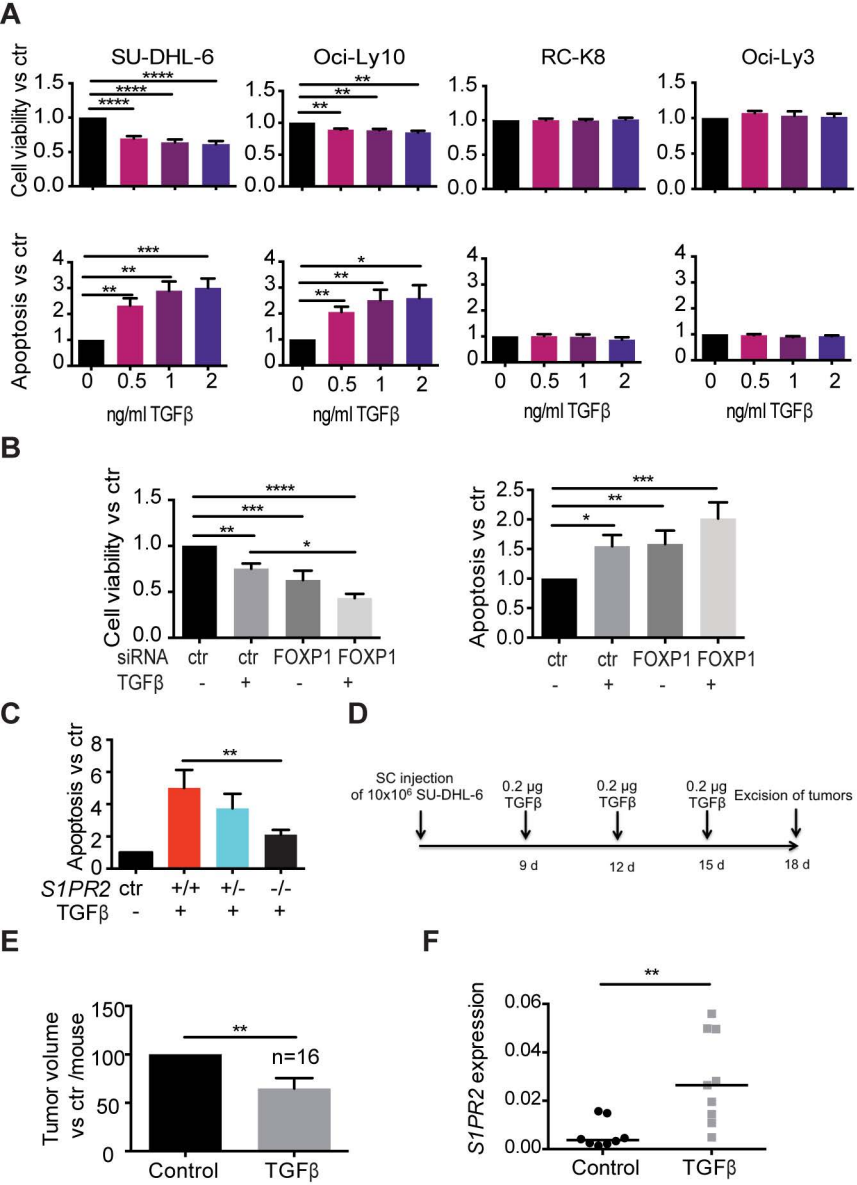
A
SU-DHL-6
Oci-Ly10
RC-K8
Oci-Ly3
Cell viability vs ctr
Apoptosis vs ctr
ng/ml TGFβ
B
Cell viability vs ctr
Apoptosis vs ctr
siRNA ctr ctr FOXP1 FOXP1
TGFβ - + - +
C
Apoptosis vs ctr
S1PR2 ctr +/+ +/- -/-
TGFβ - + + +
D
SC injection of 10x10⁶ SU-DHL-6
0.2 µg TGFβ
0.2 µg TGFβ
0.2 µg TGFβ
Excision of tumors
9 d
12 d
15 d
18 d
E
Tumor volume vs ctr /mouse
n=16
Control
TGFβ
F
S1PR2 expression
Control
TGFβ

# Figure 5

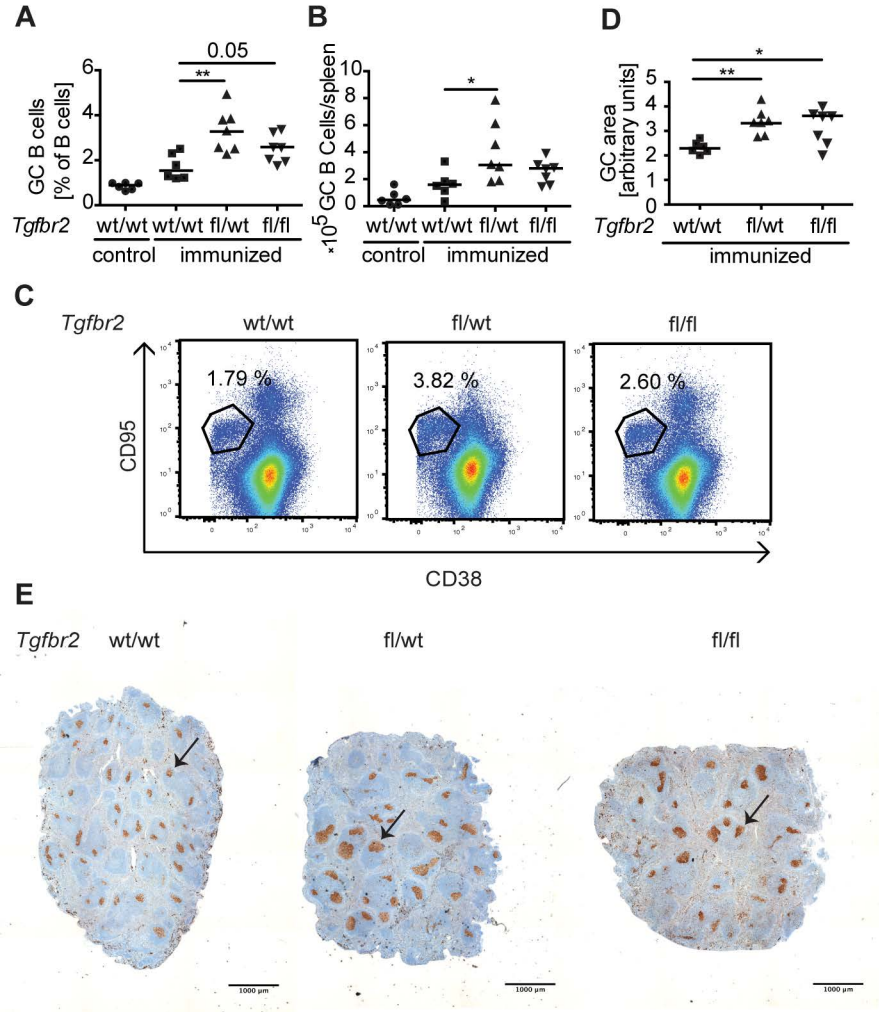
A
GC B cells [% of B cells]
0.05
**
Tgfbr2
wt/wt wt/wt fl/wt fl/fl
control
immunized
B
×10^5 GC B Cells/spleen
*
Tgfbr2
wt/wt wt/wt fl/wt fl/fl
control
immunized
D
GC area [arbitrary units]
*
**
Tgfbr2
wt/wt fl/wt fl/fl
immunized
C
Tgfbr2
wt/wt
fl/wt
fl/fl
1.79 %
3.82 %
2.60 %
CD95
CD38
E
Tgfbr2
wt/wt
fl/wt
fl/fl
1000 µm
1000 µm
1000 µm

Figure 6

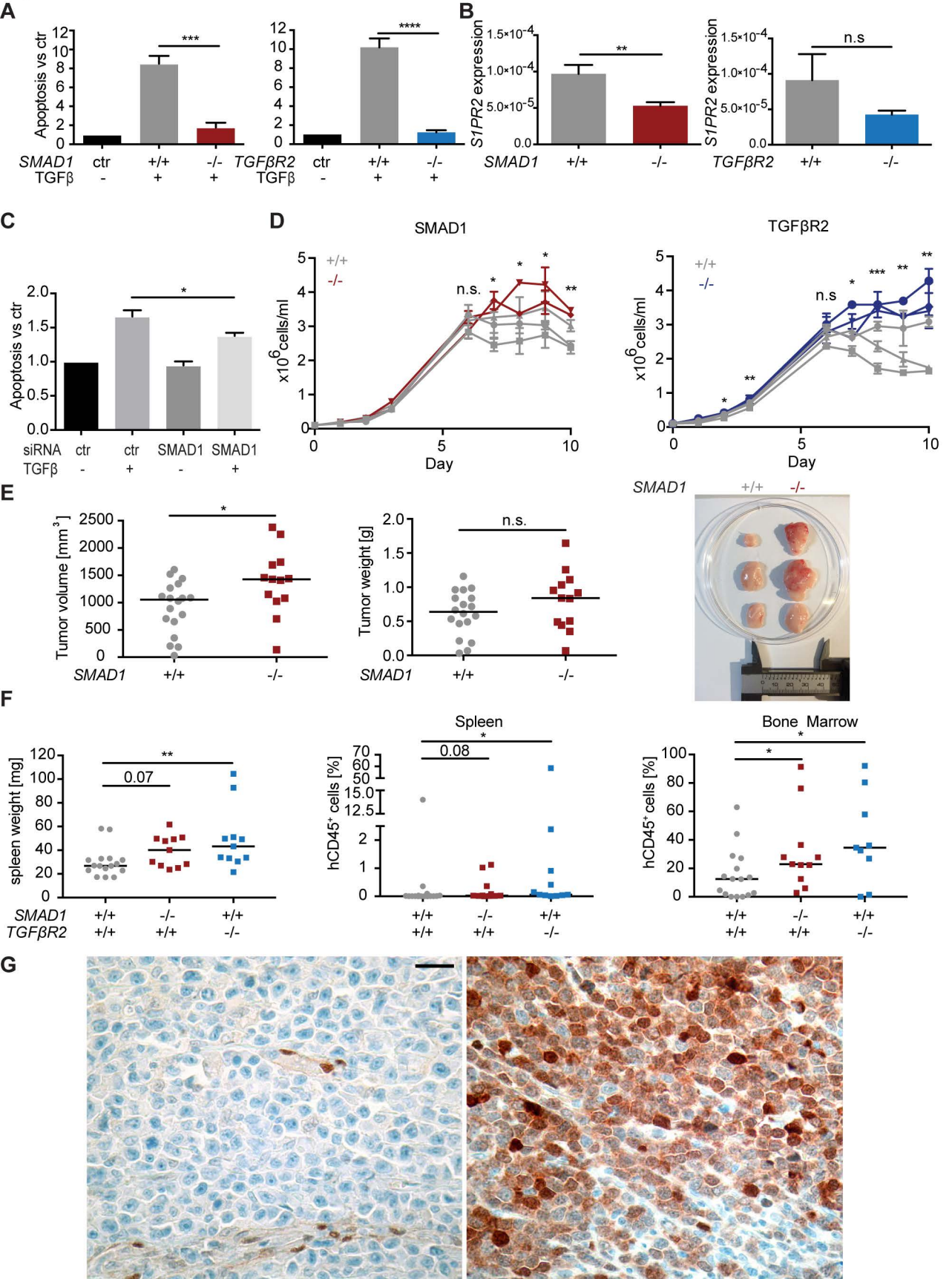
A
Apoptosis vs ctr
***
****
SMAD1 ctr +/+ -/-
TGFβ - + +
TGFβR2 ctr +/+ -/-
TGFβ - + +
B
S1PR2 expression
**
n.s
SMAD1 +/+ -/-
TGFβR2 +/+ -/-
C
Apoptosis vs ctr
*
siRNA ctr ctr SMAD1 SMAD1
TGFβ - + - +
D
SMAD1
TGFβR2
+/+
-/-
x10^6 cells/ml
n.s.
Day
E
Tumor volume [mm^3]
Tumor weight [g]
n.s.
SMAD1 +/+ -/-
F
spleen weight [mg]
0.07
Spleen
Bone Marrow
hCD45+ cells [%]
0.08
SMAD1 +/+ +/+ -/- +/+
TGFβR2 +/+ +/+ -/-
G

# Figure 7

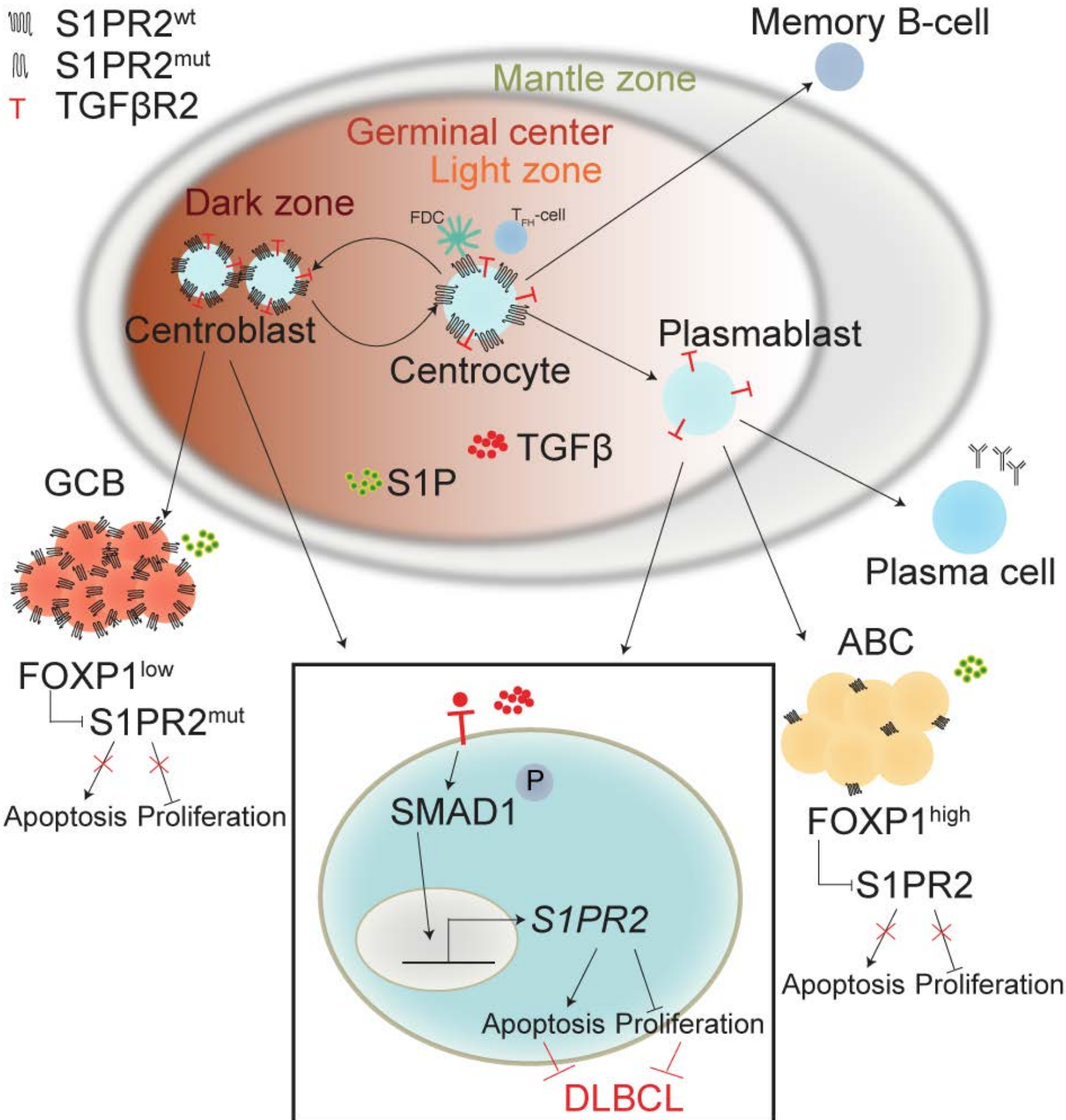
S1PR2wt
S1PR2mut
TGFβR2
Memory B-cell
Mantle zone
Germinal center
Light zone
Dark zone
FDC
TFH-cell
Centroblast
Centrocyte
Plasmablast
TGFβ
S1P
GCB
Plasma cell
ABC
FOXP1low
S1PR2mut
Apoptosis
Proliferation
SMAD1
P
S1PR2
Apoptosis
Proliferation
DLBCL
FOXP1high
S1PR2
Apoptosis
Proliferation

Prepublished online April 3, 2018;
doi:10.1182/blood-2017-10-810630

# The tumor suppressive TGF-β/SMAD1/S1PR2 signaling axis is recurrently inactivated in diffuse large B-cell lymphoma

Anna Stelling, Hind Hashwah, Katrin Bertram, Markus G. Manz, Alexandar Tzankov and Anne Müller



Blood (print ISSN 0006-4971, online ISSN 1528-0020), is published weekly by the American Society of Hematology, 2021 L St, NW, Suite 900, Washington DC 20036.